SAR Image Specle Reduction based on a Generative Adversarial Network

Ruijiao Liu
School of Artificial Intelligence
Xidian University
Xian, China
rj_liu@stu.xidian.edu.cn

Yangyang Li
School of Artificial Intelligence
Xidian University
Xian, China
yyli@xidian.edu.cn

Licheng Jiao
School of Artificial Intelligence
Xidian University
Xian, China
lchjiao@mail.xidian.edu.cn

***Abstract*—Synthetic aperture radar (SAR) image despeckling is recognized as the basis for SAR image processing and interpretation. Over the past decades, many impressed speckle reduction methods have been developed and achieved good performance under certain circumstances. However, how to suppress speckle noise in a homogeneous region while more effectively protecting details and avoid distortion of data features caused by homomorphic transformation is still an urgent problem. In this paper, a novel speckle reduction algorithm based on generative adversarial network (GAN) is proposed, which contains a generator and a discriminator. For the generator that is used directly for subsequent noise reduction, a total variation (TV) loss function is added. Meanwhile, we directly learn the mapping between the input image and the ground truth rather than the logarithmic transformation. Indeed, the improved lightweight discriminative network will also provide learning guidance for the generator. Experiments on simulatedSAR images and real SAR images demonstrate the improvement in visual and statistical performance comparing to the state-of-the-art despeckling algorithms.**

***Index Terms*—SAR image, despeckling, GAN, generator, discriminator, TV**

I. Introduction

Synthetic aperture radar (SAR) images preserve features that are not captured by optical sensors on the target scene independently of the weather and lighting conditions. These features are invaluable in remote sensing imaging applications, ranging from the analysis of the environment to urban planning and Earth monitoring [1]. However, the presence of speckle noise (shown in Fig. 1), caused by the coherent nature of the scattering, prevents many computer vision tasks (such as object detection, classification and decomposition) from achieving better performance. For instance, Medasani and Reddys research in [2] shows that the speckle noise seriously affects the accuracy of classification on radar images (RISAT -1).

To reduce the impact of speckle noise on subsequent processing and people's understanding of the image, many researchers have done a lot of effort on SAR image despeckling in the past decades. In general, traditional despeckling methods fall into two categories: spatial domain methods and transform domain methods. Spatial filtering is to directly perform data operations on the original image to process the gray value of the pixel. The Lee filter proposed in [3] is simple in the sense

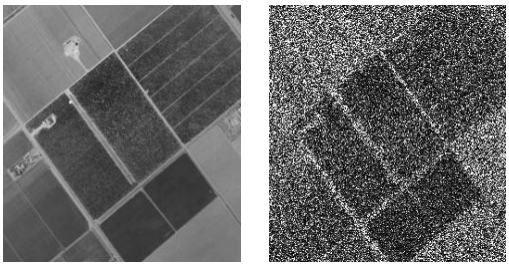

Fig. 1. Comparison of clean image and synthetic SAR image with speckle.

that it just averages those local neighborhood pixels which have the intensities within a fixed sigma range of the center pixel. Kuan filter proposed in [4] estimates the clean image by filtering pixels one by one, which local statistical characteristics of these pixels change with the different spatial location. The good self-adaptability makes the filter achieve better speckle removal effect. Frost filtering [5] is a Wiener adaptive filter with a convolution of pixel values and an exponential impulse response within a window of a certain size. These classical spatial domain methods advantages are reflected in the simple algorithm frame and good real-time performance. However, the restoration of edge details is greatly affected by the setting of local window parameters. For transform domain methods [6]–[8], denosied results are obtained by performing a certain transform (such as wavelet, Shearlet and Contourlet) on the noisy image and a corresponding inverse transform on the transform coefficients. Of course, these coefficients are processed. Though they can suppress speckles and protect edge details to some extent , above mentioned transform domain methods suffer from the increased complexity and computation.

The essence of the image denoising methods mentioned above is to unearth and utilize the correlation of images. Nonlocal means (NLM) filtering was proposed with the aim at well preserve image details by exploiting images nonlocal correlation. Inspired by the NLM filter which removes additive white Gaussian noise, some variants are then developed for processing SAR images [9] and [10], which have produced powerful and well known method is SAR block-matching 3D (SAR-BM3D) [11]. But the image priors used by these

978-1-7281-6926-2/20/$31.00 ©2020 IEEE

methods are mostly defined based on human knowledge, so it is difficult to capture all the features of the image.

In recent years, deep learning based algorithms have shown to produce stat-of-the-art on various image processing tasks. After the innovative algorithm DnCNN [12] for removing additive white Gaussian noise (AWGN) was proposed in, several algorithms for dropping speckle noise based on deep learning began to emerge. SAR-CNN [13] relies on residual learning to speed up the convergence speed under limited data sets. The framework of its network constitutes 17 full convolutional layers without pooling layer. The number of feature map and the size of filter in each layer are 64 and 33 pixels respectively. No matter whether it is evaluated from the spot removal effect or from the perspective of operating efficiency, SAR-CNN is superior compared with traditional algorithms. But the homomorphic filtering involved in SAR-CNN will seriously distort the dynamic and basic characteristics of the data, causing the despeckled image to be biased. The network structure of ID-CNN [14] also adopts the baseline proposed in [12]. Unlike SAR-CNN, it operates directly on the original noisy image, rather than take the log transform on the observed noisy image. Even though tremendous improvements have been achieved, we note that these CNN-based methods are commonly treat each pixel in the same way: optimizing the minimum Euclidean distance between a clean image and a speckled image. Actually, the perceptually meaningful information may be lost during the optimization. It is not limited to calculating the loss function with the clean image, but using the difference between it and noisy images to guide the neural network to learn the mapping relationship between clean and noisy images.

To make better use of the information of the image itself and the correlation between pixels, we propose a new speckle removal algorithm based on the Generative Adversarial Network (GAN) [15] framework. Instead of using a homomorphic transform, we directly learn the mapping between the input image and the ground truth. This GAN-based algorithm do not have to depend on human knowledge of image priors. Meanwhile, the design of the discriminator can reduce the amount of network parameters and further improve the calculation efficiency. The most important thing is that the information obtained from the discriminator can guide and fully exploit the powerful functions of the generator to make it learn from the data, thereby further improving the speckle removal performance of edge details. Extensive experiments show that the proposed method achieves significant improvements over the state-of-the-art speckle reduction algorithms.

This paper is organized as follows. A brief background of speckle noise model, GANs and perceptual loss is given in Section II. The details of the proposed method are given in Section III. Experimental results on both synthetic and real images are presented in Section IV. Finally, Section V concludes the paper with a brief summary and discussion.

II. Background

A. Speckle noise model

The information in SAR images is important for many image processing tasks and human interpretation, but speckle noise causes degradation of these images. Hence, speckle reduction is a necessary procedure. The speckle noise can typically be modelled as product of clean image pixel and multiplicative moise :

$$Y = XN \tag{1}$$

where $X \in R^{W \times H}$ and $N \in R^{W \times H}$ reprensent the speckle-free image pixel and multiplicative noise respectively. The goal is to recover X from observed image Y. One common assumption of $N \in R^{W \times H}$ is that it follows a Gamma distribution with unit mean and variance $1/L$ and has the following probability density function [16] :

$$p(N) = \frac{1}{\Gamma(L)} L^L N^{L-1} e^{-LN} \tag{2}$$

where $\Gamma(\cdot)$ denotes the Gamma function and $N \geq 0, L \geq 1$.

Speckle noise is multiplicative in nature, so the relationship between the real signal and the observed pixels is either coexist or disappear at the same time. In this article, the deep learning based GAN network is used to exploit the mapping from speckled SAR image to the clean one.

B. Generative Adversarial Network (GAN)

Recently, Generative Adversarial Network (GAN) has attracted widespread attention due to its outstanding performance. GAN was proposed to appraise generative model, which could avoid some difficult of deep learning. Generally, GAN consists of a generator and a discriminator, both of which are independent networks. The purpose of discriminator is to have the ability to distinguish between real and fake images, which should be trained many times to make it very sensitive to the generated data. However, the goal of generator is to generate a fake image which is as close as possible to the distribution of real data to fool the discriminator. Specifically, the loss function of GAN is:

$$\begin{aligned} \min_G \max_D V(D,G) = & E_{x \sim p_{data}(x)}[log(D(x)] \\ & + E_{Y \sim p_Y(y)}[log(1 - D(G(y)))] \end{aligned} \tag{3}$$

where x and $G(y)$ are the real and generated data respectively. $D(x)$ and $D(G(y))$ are distinguish results from discriminator. Indeed, the value of $D(G(y))$ that generator wants to get is larger, the better. On contrary, discriminator hopes it smaller and the value of $D(x)$ is bigger. It can be seen that these two networks are contradictory and competing with each other. The training process will not stop until the generative network captures a distribution very close to the real data.

In many researches [17]–[19], GANs show the potential to learn more complex distributions. As we all know, the training process of GAN is arduous and unstable. So there are also many improved versions of GAN, such as DC-GAN [20] and WGAN [21], [22].

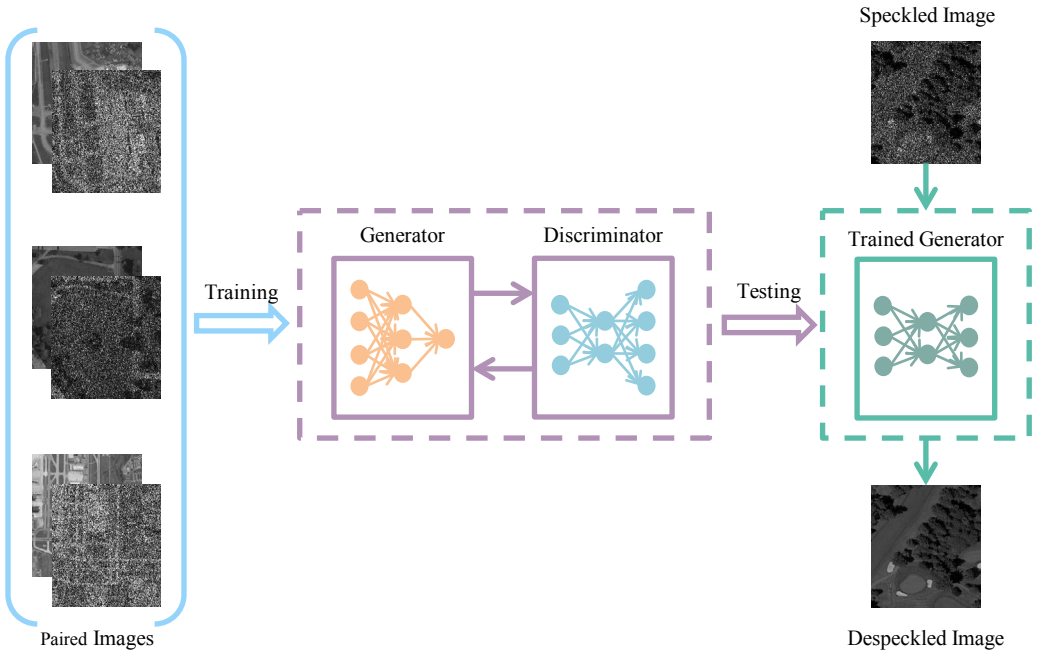

Fig. 2. Overall flowchart of the proposed algorithm.

III. Proposed Method

Instead of the logarithmic transformation in a despeckling framework, we aim to directly learn a mapping from an input speckled image to a de-speckled (background) image by constructing a GAN-based deep network. The proposed algorithm is composed of two networks: a generator sub-network G, a discriminator sub-network D. Fig. 2 shows the structure of the proposed method. The generator subnet is a deep convolutional neural network, which shown in Fig 3. Its primary task is to synthesize a clean SAR image without speckles from a speckle-polluted image (input speckled SAR image). The discriminator sub-network D, as shown in Fig. 3, serves to distinguish the fake images generated from sub-network G from corresponding ground truth real image. In this way, the excellent distinguish ability of D can give G a better learning direct.

A. Network Architecture Design

The generator network G aims to map speckled SAR images to the clean image. Speckles can be removed when the generator is trained. G starts with a convolutional layer with 64 filters, size 3 3 and stride 1, along with ReLU action function. Meanwhile, appropriate zero-padding to make sure that the output of each layer shares the same dimension with that of the input image. Then, six identical convolution layers with the same number and size of filters as the first layer are used consecutively. The difference is that these six convolutional layers have an additional batch normalization between convolution and ReLU. Next, the eighth layer is the same with the first layer in all aspects. Before the finally output, tanh activation layer is performed.

According to the generating result, the task of the discriminator network D is compresses the image into a confidence value. Different from the conventional discriminator network proposed in [23], we use 70 70 PatchGAN [24]. It not only has fewer parameters, but also can be applied to images of any size. The architecture of D is four stride convolutional blocks. The kernel size and stride are 3 3 and 2 respectively, which are the same in the four blocks. The filter numbers of them is 64, 128, 256 and 512. Finally, the fully-connected layer project the feature vector to a confidence value whether the image is real or fake. Leakey ReLU with slope = 0.2 is used after each instance normalization layer.

B. Loss Function

Previous works on CNN-based image restoration optimized over pixel wise L2-norm (Euclidean loss) or L1-norm between the predicted and ground truth images. In particular, for capturing images with sharper edges and details edge, the generative network is trained in an end-to-end fashion using a combination of Euclidean loss and TV loss. The new loss function is defined as follows

$$L_G = L_E + \lambda_{TV} L_{TV} \tag{4}$$

where λ_{TV} is pre-defined weights for TV loss. L_E and L_{TV} represent the normal per-pixel Euclidean loss function and additional TV loss respectively. These two loss are defined as follows

$$L_E = \frac{1}{WH} \sum_{w=1}^{W} \sum_{h=1}^{H} \left\| \phi_G(Y^{w,h}) - X^{w,h} \right\|_2^2 \tag{5}$$

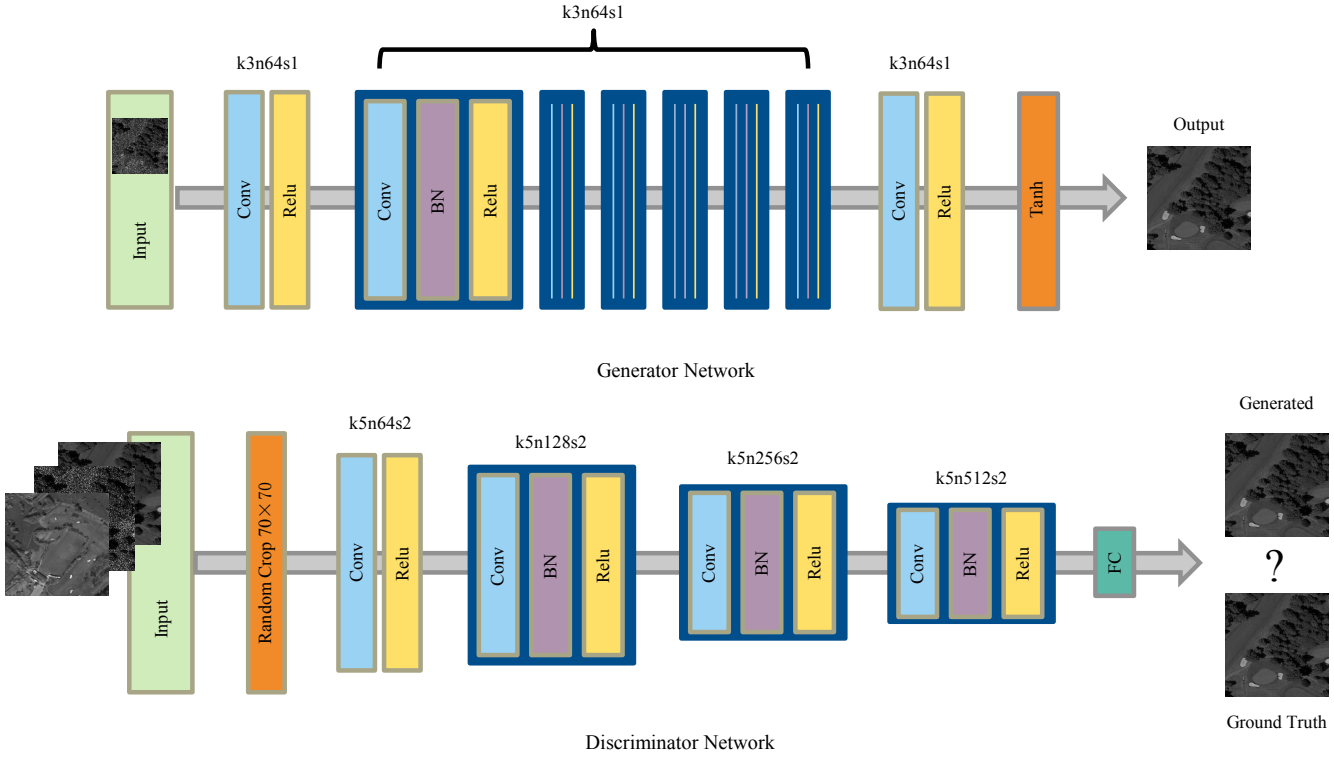

Fig. 3. Network Architectures of the generator and the discriminator.

$$L_{TV} = \sum_{w=1}^{W}\sum_{h=1}^{H}\sqrt{\left(\hat{X}^{w+1,h} - \hat{X}^{w,h}\right)^2 + \left(\hat{X}^{w,h+1} - \hat{X}^{w,h}\right)^2} \tag{6}$$

where ϕ_G is the leaned parameters of generator G for generating the despeckled image and $\hat{X} = \phi_G(Y^{w,h})$. The size of Y and X are $W \times H$.

Finally, we use this framework proposed in [25] to handle the problem of SAR image despeckling. Here we let $s = \{P_Y, P_X\}$, $t = \{P_Y, P_{\hat{X}}\}$, where P_X, P_Y and $P_{\hat{X}}$ are represent the patch from clean SAR image, speckled SAR image and $P_{\hat{X}} = G(P_Y)$ respectively. Finally, the adversarial loss L_D can be expressed as

$$L_D = \max_D E[log(D(s)) + \log(1 - D(t))] \tag{7}$$

C. Algorithm Flow

The full loss function of our algorithm is:

$$L = L_D + \lambda L_G \tag{8}$$

where L_D and L_G are adversarial loss and general loss, λ is a hyper parameter set as 100. Training procedure is shown in **Algorithm 1**.

Algorithm 1: Training procedure of our algorithm. The optimization method is Adam.

input: Speckled images Y and clean images X.

output: Parameters of generator and discriminator: θ, ω.

for numbers of training iterations **do**

1. Sample m batch clean images P_X and speckled images P_Y.

2. $P_{\hat{X}} \leftarrow G_\theta(P_Y)$

3. Concatenate $\{P_Y, P_X\}$, $\{P_Y, P_{\hat{X}}\}$ be s and t respectively

4. $L_D \leftarrow \frac{1}{m}\sum_1^m [log(D_\omega(s)) + log(1 - D_\theta(t))]$

5. Update the discriminator D by $Adam(\omega, L_D, \alpha)$

6. $L_G \leftarrow \frac{1}{m}\sum_1^m [log(D_\omega(s)) + log(1 - D_\theta(t))]$
$+\lambda\frac{1}{m}\sum_1^m (L_E + \lambda_{TV} L_{TV})$

7. Update the discriminator G by $Adam(\theta, L_G, \alpha)$

end for

IV. Experimental Results

In this section, we exhibit the experiment results of our algorithm on both synthetic and real SAR images. Comparing our method with other five excellent despeckling algorithms: Lee filter [3], Kuan filter [5], SAR-BM3D [11], SAR-CNN [13] and ID-CNN [14]. The last two are algorithms

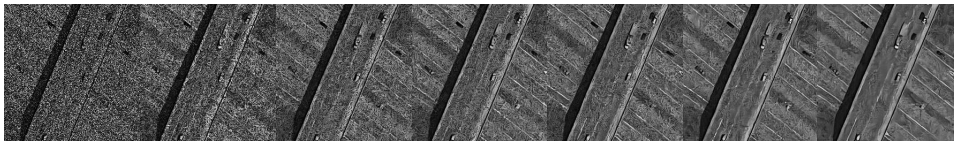

Overpass63 with L=1

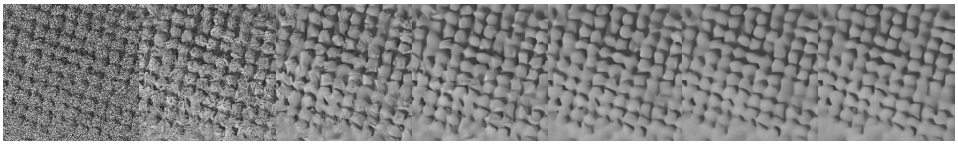

Agricultural04 with L=4

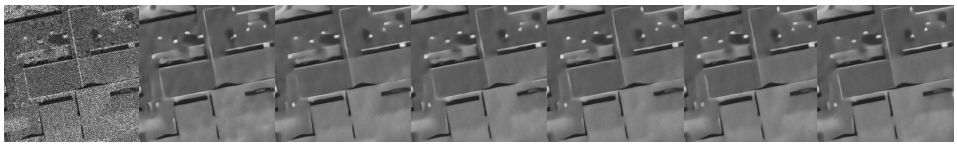

Buildings85 with L=10

Fig. 4. Visual effect on different synthetic SAR images with different looks. From left to right: SAR images, Lee, Kuan, SAR-CNN, ID-CNN and ours.

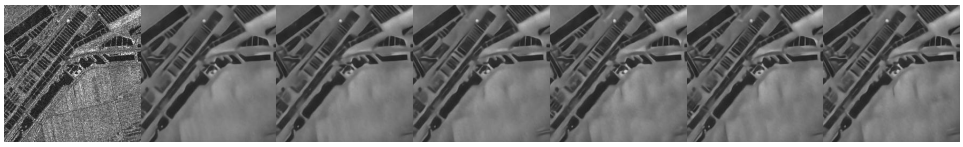

Fig. 5. Visual effect on the real SAR image. From left to right: SAR images, Lee, Kuan, SAR-CNN, ID-CNN and ours.

based on deep learning, others are traditional algorithms. For all the compared methods, parameters are set as suggested in their corresponding papers. In more detail, these algorithms are compared in two areas: visual effects and objective statistical effects, which involves the Peak Signal to Noise Ratio (PSNR) and Structural Similarity Index (SSIM). The larger the value of these two evaluation indicators, the better.

The method proposed in this paper consists training stage and testing stage, which needs a large number of pictures. The datasets we used are 400 Berkeley segmentation dataset (BSD) images [25] and 2100 UC Merced Land Use [26]. However, due to the lack of real clean SAR images, we synthesized 2500 image pairs (256×256) in the manner of Functions (1) and (2). The entire network is trained for 200 epochs by using the adaptive moment estimation (ADAM) optimization method [27], with learning rate of 1e-8. During training, the regularization parameter λ_{TV} is set equal to 0.002 and λ is 100. Then, we perform different tests in synthetic images and real SAR images respectively.

A. Results on Simulated SAR Images

We randomly selected 60 speckled images out of the 2500 images as the testing dataset. The remaining 2440 images are used for training the proposed network. And experiments are carried on different numbers of look L (L=1, 4, 10) The visual effect on different methods are shown in Fig. 4. And Tab. 1 reports PSNR and SSIM values for some out-of-training images and the algorithm proposed by us.

TABLE I
PSNR AND SSIM RESULTS ON SYNTHETIC SAR IMAGES

Look	Metric	Lee	Kuan	SAR-BM3D	SAR-CNN	ID-CNN	Ours
L=1	PSNR	21.48	21.95	22.99	23.59	24.74	**25.26**
	SSIM	0.511	0.592	0.692	0.640	0.727	**0.746**
L=4	PSNR	22.12	22.84	24.96	26.20	26.89	**26.91**
	SSIM	0.555	0.650	0.782	0.771	**0.818**	0.740
L=10	PSNR	22.30	23.11	26.45	27.63	28.07	**28.65**
	SSIM	0.571	0.671	0.834	0.825	0.853	**0.868**

As can be seen from Fig. 4the Overpass63, Agricultural04 and buildings85 are randomly selected to be simulated with the looks are set 1, 4 and 10 respectively. From the first column to the last column are the noisy SAR image and the despeckling results of Lee, Kuan, SAR-BM3D, SAR-CNN, ID-CNN and ours respectively. For the three filter-based methods, SAR-BM3D can get clear edge than the first two methods. But comparing with deep learning based methods, the edge and details have some artificial effects. In most cases, whether smooth area or edge are, our algorithm has the art-of-the-state results in vision. The smooth areas are more smoother and the edge areas become shaper in some extent.

Meanwhile, as can be seen from Tab. I, the value of PSNR can reflect that the same good results can be obtain in the case of severe speckle pollution. The most of our SSIM values are the best, except when the looks equal to 4. This demonstrate the restoration ability of our algorithm is also excellent. These experiment clearly shows the significance of the proposed image despeckling generative adversarial network as well as the use of TV loss for image despeckling.

B. Results on Real SAR Images

Due to the absence of true clean SAR image, visual inspection is the only way to qualitatively evaluate the performance of different methods. The despeckled images corresponding to the real image are shown in Fig. 5. And the sequence is the same as that of Figure 4. The first one is the original SAR image and from the second to the last one are the results of Lee, Kuan, SAR-BM3D, SAR-CNN, ID-CNN and ours respectively. We can see that more clear textures emerge in SAR-CNN, ID-CNN and ours while Lee, Frost and SAR-BM3D suffer from some blurring. It is also evident from these figures that deep-learning based methods can restore the real image details to a great extent.

V. Conclusion

We have proposed a new speckle reduction method for SAR image based on GANs framework. The generator is added a TV loss to protect image details. And use a lightweight discriminator network to guide generator and further improve the calculation efficiency. Meanwhile, compared with filtering-based algorithms and other deep-learning based methods, our algorithm performs even better both visually and statistically.

Acknowledgment

This work was supported in part by the National Natural Science Foundation of China under Grants 61772399, U1701267, 61773304, 61672405, and 61772400, in part by the Key Research and Development Program in Shaanxi Province of China under Grant 2019ZDLGY09-05, in part by the Program for Cheung Kong Scholars and Innovative Research Team in University under Grant IRT_15R53, and in part by the Technology Foundation for Selected Overseas Chinese Scholar in Shaanxi under Grants 2017021 and 2018021.

References

[1] M. L. R. Sarker, J. Nichol, H. B. Iz, B. Bin Ahmad, and A. A. Rahman, Forest Biomass Estimation Using Texture Measurements of High-Resolution Dual-Polarization C-Band SAR Data, vol. 51, no. 6, pp. 33713384, 2013.

[2] S. Medasani and G. U. Reddy, Speckle Filtering and its Influence on the Decomposition and Classification of Hybrid Polarimetric Data of RISAT-1, vol. 10, 2018.

[3] J. Sen Lee, Speckle analysis and smoothing of synthetic aperture radar images, Comput. Graph. Image Process., vol. 17, no. 1, pp. 2432.

[4] D. Kuan, A. Sawchuk, T. Strand, and P. Chavel, Adaptive restoration of images with speckle, IEEE Trans. Acoust. Speech Signal Process., vol. 35, no. 3, pp. 373383, 2003.

[5] V. S. Frost, J. A. Stiles, K. S. Shanmugan, and J. C. Holtzman, A Model for Radar Images and Its Application to Adaptive Digital Filtering of Multiplicative Noise, IEEE Trans. Pattern Anal. Mach. Intell., vol. PAMI-4, no. 2, pp. 157166, 1982.

[6] H. Guo, J. E. Odegard, M. Lang, R. A. Gopinath, I. W. Selesnick, and C. S. Burrus, Wavelet based speckle reduction with application to SAR based ATD/R, in Proceedings of 1st International Conference on Image Processing, 1994, vol. 1, pp. 7579.

[7] A. Achim, P. Tsakalides, and A. Bezerianos, SAR image denoising via Bayesian wavelet shrinkage based on heavy-tailed modeling, IEEE Trans. Geosci. Remote Sens., vol. 41, no. 8, pp. 17731784, 2003.

[8] T. Bianchi, F. Argenti, and L. Alparone, Segmentation-based MAP despeckling of SAR images in the undecimated wavelet domain, IEEE Trans. Geosci. Remote Sens., vol. 46, no. 9, pp. 27282742, 2008.

[9] C.-A. Deledalle, L. Denis, G. Poggi, F. Tupin, and L. Verdoliva, Exploiting patch similarity for SAR image processing: the nonlocal paradigm, IEEE Signal Process. Mag., vol. 31, no. 4, pp. 6978, 2014.

[10] G. Di Martino, M. Poderico, G. Poggi, D. Riccio, and L. Verdoliva, Benchmarking framework for SAR despeckling, IEEE Trans. Geosci. Remote Sens., vol. 52, no. 3, pp. 15961615, 2013.

[11] S. Parrilli, M. Poderico, C. V. Angelino, and L. Verdoliva, A nonlocal SAR image denoising algorithm based on LLMMSE wavelet shrinkage, IEEE Trans. Geosci. Remote Sens., vol. 50, no. 2, pp. 606616, 2011.

[12] K. Zhang, W. Zuo, Y. Chen, D. Meng, and L. Zhang, Beyond a gaussian denoiser: Residual learning of deep cnn for image denoising, IEEE Trans. Image Process., vol. 26, no. 7, pp. 31423155, 2017.

[13] G. Chierchia, D. Cozzolino, G. Poggi, and L. Verdoliva, SAR image despeckling through convolutional neural networks, in 2017 IEEE International Geoscience and Remote Sensing Symposium (IGARSS), 2017, pp. 54385441.

[14] P. Wang, H. Zhang, and V. M. Patel, SAR image despeckling using a convolutional neural network, IEEE Signal Process. Lett., vol. 24, no. 12, pp. 17631767, 2017.

[15] I. Goodfellow et al., Generative adversarial nets, in Advances in neural information processing systems, 2014, pp. 26722680.

[16] F. Ulaby, M. C. Dobson, and J. L. lvarez-Prez, Handbook of radar scattering statistics for terrain. Artech House, 2019.

[17] H. Zhang, V. Sindagi, and V. M. Patel, Image de-raining using a conditional generative adversarial network, IEEE Trans. circuits Syst. video Technol., 2019.

[18] C. Ledig et al., Photo-realistic single image super-resolution using a generative adversarial network, in Proceedings of the IEEE conference on computer vision and pattern recognition, 2017, pp. 46814690.

[19] F. Liu, L. Jiao, and X. Tang, Task-Oriented GAN for PolSAR Image Classification and Clustering, IEEE Trans. Neural Networks Learn. Syst., pp. 113, 2019.

[20] A. Radford, L. Metz, and S. Chintala, Unsupervised representation learning with deep convolutional generative adversarial networks, arXiv Prepr. arXiv1511.06434, 2015.

[21] M. Arjovsky, S. Chintala, and L. Bottou, Wasserstein gan, arXiv Prepr. arXiv1701.07875, 2017.

[22] I. Gulrajani, F. Ahmed, M. Arjovsky, V. Dumoulin, and A. C. Courville, Improved training of wasserstein gans, in Advances in neural information processing systems, 2017, pp. 57675777.

[23] P. Wang, H. Zhang, and V. M. Patel, Generative adversarial network-based restoration of speckled SAR images, in 2017 IEEE 7th International Workshop on Computational Advances in Multi-Sensor Adaptive Processing (CAMSAP), 2017, pp. 15.

[24] C. Li and M. Wand, Precomputed real-time texture synthesis with markovian generative adversarial networks, in European Conference on Computer Vision, 2016, pp. 702716.

[25] Y. Chen and T. Pock, Trainable nonlinear reaction diffusion: A flexible framework for fast and effective image restoration, IEEE Trans. Pattern Anal. Mach. Intell., vol. 39, no. 6, pp. 12561272, 2016.

[26] Y. Yang and S. Newsam, Bag-of-visual-words and spatial extensions for land-use classification, in Proceedings of the 18th SIGSPATIAL international conference on advances in geographic information systems, 2010, pp. 270279.

[27] [1] D. P. Kingma and J. Ba, Adam: A method for stochastic optimization, arXiv Prepr. arXiv1412.6980, 2014.